Electronic structure and chemical bonding of the first row transition metal dichlorides, $MnCl_2$, $NiCl_2$, and $ZnCl_2$: A high resolution photoelectron spectroscopic study

Lai-Sheng Wang, B. Niu, Y. T. Lee, and D. A. Shirley
Department of Chemistry, University of California at Berkeley and Materials and Chemical Sciences Division, Lawrence Berkeley Laboratory, Berkeley, California 94720

(Received 26 February 1990; accepted 12 April 1990)

High resolution He I (584 Å) photoelectron spectra of $ZnCl_2$, $MnCl_2$, and $NiCl_2$ were measured using a high temperature supersonic molecular beam source. In $ZnCl_2$, vibrational structures were resolved, and spectroscopic constants were derived for the observed molecular ion states. A single ν_1 vibrational progression was observed for the $C\,^2\Sigma_g^+$ state of $ZnCl_2^+$. A Franck–Condon factor calculation allowed us to obtain a Zn–Cl equilibrium bond length increase of 0.095(5) Å and a ν_1 vibrational frequency of 290(8) cm^{-1}. For the open-shell molecules, $MnCl_2$ and $NiCl_2$, no vibrational structure could be resolved because of their very low bending frequencies. Transitions from the ligand orbital and metal *d* orbital ionizations were clearly resolved, with those of the *d* orbitals having considerably narrower band widths. Even though many final states are expected for ionization of the open-shell *d* orbitals, only a few states were observed. This was explained in $MnCl_2$ by the one-electron spin selection rule: $S_f = S_i \pm 1/2$. Besides the spin selection rule, a propensity toward high spin was proposed to account for the spectrum of $NiCl_2$. From the metal *d* orbital and ligand orbital splittings, the degree of covalent bonding was inferred to be in the order of: $MnCl_2 > NiCl_2 > ZnCl_2$.

I. INTRODUCTION

The first row transition metals are the lightest elements in the Periodic Table for which the free atoms have *d* orbitals that must be taken into account in chemical bonding. These *d* orbitals often impart interesting chemical and physical properties to the transition metal compounds.[1] Even though the first row transition metal dihalides are among the simplest transition metal compounds which can be studied as free molecules, they are still difficult to study and are incompletely characterized spectroscopically. Still, much remains to be understood about these compounds. There have been earlier infrared[2,3] and ultraviolet[4–6] absorption studies both in the gas phase and in rare gas matrices, and electron diffraction studies[7] to determine the geometric structure. The dichlorides are now known to be linear and symmetric[7,8] with a very small bending frequency.[3,9]

Theoretically, these molecules are difficult subjects too, because of their open-shell character and the large number of electrons involved. Electron correlation, spin–orbit, and spin–spin effects should be taken into account, and large basis sets are required. Consequently, there have been few *ab initio* quantum chemical calculations on these molecules.[10–12]

There is also considerable discussion about the degree to which the *d* orbitals participate in chemical bonding, particularly in the transition metal dimers which have drawn great interest recently within the chemical physics community in the context of studying transition metal clusters. It was believed that when two transition metal atoms formed a diatomic molecule the bonding involved mainly the 4*s* orbitals, while the 3*d* orbitals were largely localized on the two atoms. The unpaired *d* electrons on the two atoms could couple to form many low-lying excited states. Indeed, just for the Fe_2 molecule alone, Shim and Gingerich[13] have predicted that 112 states would lie within about 0.6 eV above the ground state. However, in a Fe_2^- negative ion photodetachment experiment recently by Leopold and Lineberger,[14] only two pronounced bands were observed within about 0.6 eV above the Fe_2 ground state. Based on this observation, the authors tentatively concluded that the 3*d* orbitals were more strongly bound in Fe_2 than previously thought and hence did not produce a large number of low-lying excited states through the weak *d–d* coupling. It is now known that there is considerable *d* orbital bonding in the first row transition metal dimers on the left side of the Periodic Table and that this bonding gets weaker across the Periodic Table from left to right.

The bonding situation in the transition metal dichlorides is different from that in the transiton metal dimers. Nevertheless, these molecules also have open-shell 3*d* orbitals, and the unpaired 3*d* electrons can in principle couple to give many final states upon photoionization. The small number of final states evident in the Fe_2^- negative ion photodetachment experiment enhances the interest of a high resolution photoelectron spectroscopic study of the transition metal dichlorides. An initial question is: can we observe all the predicted final states in the photoelectron spectra of the transition metal dichlorides?

There have been three previous photoelectron spectroscopic investigations of the first row transiton metal dichlorides.[15–17] Unfortunately, due in part to the limited resolution in these studies, the spectral assignments have not been consistent.

We have recently built a high temperature molecular beam source,[18–20] which is especially suitable to study these

 0021-9606/90/140957-10$03.00

molecules with high resolution. We are also interested in resolving vibrational structures in the photoelectron spectra of these molecules. These would provide important information about the chemical bonding and a better spectroscopic characterization of the molecular ions. It is also our hope that these experimental studies can spur more theoretical interest[21] on these relatively simple transition metal complexes.

Zinc, with a closed $3d$ shell, is not considered to be a transition metal. However, $ZnCl_2$ is a much simpler molecule in terms of electronic structure, and has been better understood than the transition metal dihalides. There have been numerous photoelectron spectroscopic investigations of $ZnCl_2$ at low resolution,[22–27] none of which has resolved any vibrational structure. Besides the interest in studying $ZnCl_2$ at higher resolution, we include it in this study as a comparison with the more complicated transition metal molecules, $MnCl_2$ and $NiCl_2$.

II. EXPERIMENTAL

The experiments were performed with a newly constructed high temperature molecular beam source, recently described elsewhere.[18–20] Only a brief description, and features related to the current experiments will be given here. The source used electron-bombardment heating and a graphite crucible, and it had the capability to entrain carrier gases to produce seeded supersonic beams of high temperature species with internal cooling. The experimental conditions for each experiment are listed in Table I.

Thermodynamically, $ZnCl_2$, $MnCl_2$, and $NiCl_2$ are known to evaporate mainly as monomers.[28–31] All samples were purchased from Johnson Matthey Inc., $NiCl_2$ in its hydrated form, and $ZnCl_2$ and $MnCl_2$ in their anhydrous forms. These materials are extremely hygroscopic, and were all dried before use. Moreover, each sample underwent prolonged heating at a temperature below its melting point in vacuum to be dehydrated further. Even with these efforts, small amounts of water and hydrogen chloride, due to the reaction of water with the metal dichlorides, were still observable at the beginning of each experiment. In the case of $ZnCl_2$, minute amounts of these impurities persisted during the full course of the experiment, due to the lower temperature needed for the evaporation. In the cases of $MnCl_2$ and $NiCl_2$, these impurities disappeared shortly after the operating temperatures were reached.

It was not necessary to have absolutely accurate temperature measurements in these experiments. In general, about 1–5 Torr vapor was needed to be able to collect a spectrum. Both a quadrupole mass spectrometer and the photoelectron spectrometer were used to monitor the evaporation process. Once a reasonable photoelectron count level was reached, the temperature was stabilized and the whole experiment was done at this temperature. The beam source pressure was kept below 5×10^{-4} Torr during an experiment. The carrier gas pressure was adjusted to maintain this vacuum in the beam source.

Special care had to be exercised for running $ZnCl_2$ and $MnCl_2$ because they were evaporated above their melting points. It was found that the carrier gas could spill the liquid samples in the graphite crucible and make liquid jets. Special quartz sample cells had to be used to confine the liquid samples inside the crucible in these cases, as shown in Fig. 1. The two openings (6.35 mm diameter holes) in the cell always faced up. $NiCl_2$ had a high enough sublimation pressure below its melting point, and was loaded into the graphite crucible directly without using a sample cell.

TABLE I. Experimental conditions.

	$ZnCl_2$	$MnCl_2$	$NiCl_2$
T(K)[a]	800	1000	960
P(Torr)[b]	110 (He)	120 (He)	500 (He)
ϕ(mm)[c]	0.18	0.23	0.16
Power (mA×V)[d]	30×600	200×600	60×1200
Starting materials	Pure $ZnCl_2$	Pure $MnCl_2$	Pure $NiCl_2$

[a] Accuracy of temperature measurements was ± 50 K.
[b] Carrier gas pressure.
[c] Nozzle diameters.
[d] Heating power, emission current (mA) times applied high voltage (V). About 60 W power was needed to drive the tungsten filament, which is in addition to the heating power.

The details of the photoelectron spectrometer have also been published previously.[32] Briefly, it consists of a helium discharge lamp as the photon source (584 Å), a quadrupole mass spectrometer and a hemispherical electron energy analyzer with a multichannel detector. The energy resolution of the anlayzer was about 12 meV, as measured with the $Ar^+P_{3/2}$ photoelectron peak which was used for calibration. Under high temperature conditions, drift of the energy scale was severe, and shorter scans were taken and the spectra were later added to enhance the counting statistics. As a result, the effective resolution in the final spectra was about 15 meV.

III. RESULTS AND DISCUSSION

A. General remarks

Before discussing the spectra, let us first examine the molecular orbitals and the chemical bonding in the first row transition metal dichlorides. It is generally believed that the participation of the $3d$ orbitals in chemical bonding decreases from the left to the right side of the Periodic Table. For Zn, a closed shell element, the $3d$ orbitals should be core-like, with little bonding capability. Ligand field theory[33,34] has been used to describe the chemical bonding in these mol-

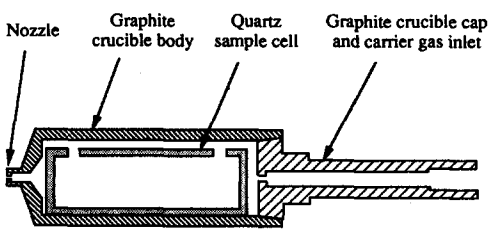

FIG. 1. The graphite crucible configuration with a sample cell.

ecules. In this theory, we allow the two Cl^- ligands to approach the central metal ion M^{2+} collinearly and split the fivefold degenerate d orbitals into σ_g, π_g, and δ_g orbitals. The ligands can backtransfer charge to the $3d$ orbitals, facilitating covalent bonding character between the ligands and the central metal atom. Obviously, there cannot be any back transfer in $ZnCl_2$, and the bonding should be primarily electrostatic. The valence molecular orbitals can be written as follows:

$$\delta_g \pi_g \sigma_g \quad \sigma_g \sigma_u \pi_u \pi_g$$

$$(3d) \qquad (\mathrm{Cl}\ 3p)$$

where only the Cl $3p$ and the metal-atom $3d$ orbitals are shown. The first three orbitals (δ_g, π_g, and σ_g) are mainly from the metal atom $3d$ orbitals and the later four (σ_g, σ_u, π_u, and π_g) are mainly from the Cl $3p$ orbitals. A schematic pictorial representation of these orbitals is shown in Fig. 2. For the closed-shell $ZnCl_2$ molecule, the above orbital sequence is correct, with the $3d$ orbitals being almost corelike. However, the situations are more complicated for $MnCl_2$ and $NiCl_2$, where the $3d$ orbitals are only partially filled. It is now fairly well established that the ground states of these molecules assume the states of maximum multiplicity[4,5,10] just as in the free atoms and ions. Therefore, we have the following valence electronic configurations for the ground states of $ZnCl_2$, $MnCl_2$, and $NiCl_2$:

$$\cdots 1\delta_g^4 2\pi_g^4 8\sigma_g^2 9\sigma_g^2 7\sigma_u^2 4\pi_u^4 2\pi_g^4 \quad {}^1\Sigma_g^+ \quad ZnCl_2,$$

$$\cdots 8\sigma_g^2 7\sigma_u^2 4\pi_u^4 2\pi_g^4 1\delta_g^2 3\pi_g^2 9\sigma_g^1 \quad {}^6\Sigma_g^+ \quad MnCl_2,$$

$$\cdots 8\sigma_g^2 7\sigma_u^2 4\pi_u^4 2\pi_g^4 1\delta_g^4 3\pi_g^3 9\sigma_g^1 \quad {}^3\Pi_g \quad NiCl_2.$$

To avoid confusion in later discussions, we numbered each molecular orbital by counting the inner orbitals. It is to be noted that the $1\delta_g$, $2\pi_g$, and $8\sigma_g$ orbitals correspond to the $3d$ orbitals in $ZnCl_2$, while the $1\delta_g$, $3\pi_g$, and $9\sigma_g$ orbitals correspond to the $3d$ orbitals in $MnCl_2$ and $NiCl_2$. The rest of the orbitals corresponds to the Cl $3p$ orbitals. The orbitals omitted in the above all have ionization potentials too high to show up in the He I (584 Å) photoelectron spectrum.

The closed-shell configuration of $ZnCl_2$ implies a simple photoelectron spectrum from a one-electron point of view. Ionization of each orbital produces one photoelectron band, neglecting spin–orbit splittings. However, the situations are much more complicated in $MnCl_2$ and $NiCl_2$ because of the open d shell. Table II lists all the possible final states upon d-electron ionization in $MnCl_2$ and $NiCl_2$, assuming Russell–Saunders coupling.[35] There are indeed many possible final states for each one-electron ionization, except for the $9\sigma_g$ orbital in $NiCl_2$. It should be interesting to see how or whether all these final states will show up in the photoelectron spectra. For each ligand-orbital ionization there would be also a large number of possible final states because of the presence of the unpaired d electrons. We assume that the coupling between the ligand orbital electrons and the $3d$ electrons is weak, and we shall not consider it here. In other words, we should still expect only one band for each ligand ionization. In the following, we shall first discuss the $ZnCl_2$ spectrum and then proceed to $MnCl_2$ and $NiCl_2$.

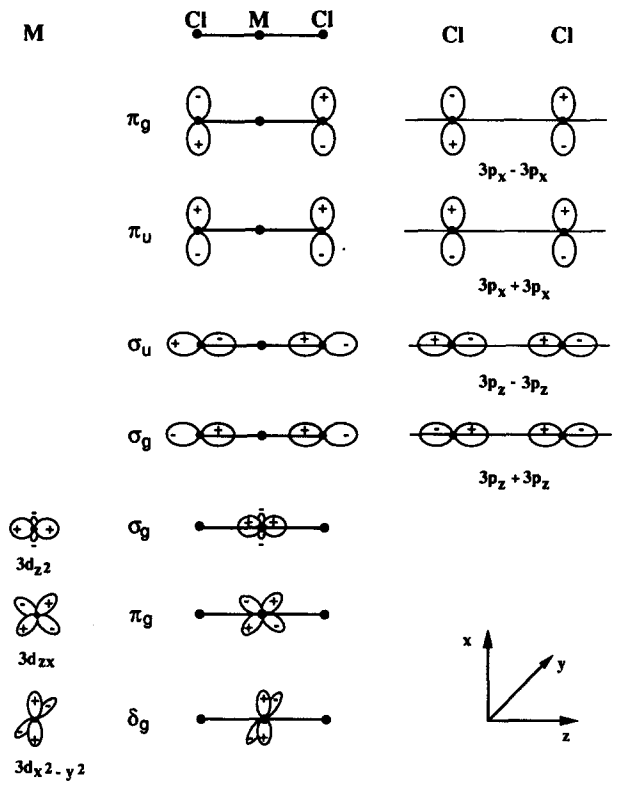

FIG. 2. A schematic pictorial representation of the valence molecular orbitals of a linear MCl_2 molecules (M = first row transition metals, Cu and Zn). Only one component is drawn for the π_g and π_u orbitals of the ligands, and for the π_g and δ_g orbitals of the central metal atom.

B. $ZnCl_2$

The photoelectron spectrum of $ZnCl_2$ has been extensively studied and the spectral assignments are well established.[22–27] The ground stae vibrational frequencies[36] of $ZnCl_2$ are $\omega_e(\nu_1) = 358\ \mathrm{cm}^{-1}$, $\omega_e(\nu_2) = 295\ \mathrm{cm}^{-1}$, and $\omega_e(\nu_3) = 516\ \mathrm{cm}^{-1}$. These are well within our experimental resolution. We should be able to resolve vibrational struc-

TABLE II. Terms of electron configurations after removing a d electron in $MnCl_2$ and $NiCl_2$.

Orbitals ionized	Electron configuration	Molecular electronic terms
	$MnCl_2$: $\cdots 8\sigma_g^2 7\sigma_u^2 4\pi_u^4 2\pi_g^4 1\delta_g^2 3\pi_g^2 9\sigma_g^1$	${}^6\Sigma_g^-$
$9\sigma_g^{-1}$	$\cdots 1\delta_g^2 3\pi_g^2$	${}^5\Sigma_g^-, {}^3\Sigma_g^-(2), {}^3\Delta_g, {}^3\Gamma_g, {}^1\Sigma_g^+(2), {}^1\Delta_g(2), {}^1\Gamma_g, {}^1\mathrm{I}_g$
$3\pi_g^{-1}$	$\cdots 1\delta_g^2 3\pi_g^1 9\sigma_g^1$	${}^5\Pi_g, {}^3\Pi_g(2), {}^3\Phi_g, {}^3\mathrm{H}_g, {}^1\Pi_g(2), {}^1\Phi_g, {}^1\mathrm{H}_g$
$1\delta_g^{-1}$	$\cdots 1\delta_g^1 3\pi_g^2 9\sigma_g^1$	${}^5\Delta_g, {}^3\Sigma_g^+, {}^3\Sigma_g^-, {}^3\Delta_g(2), {}^3\Gamma_g, \Sigma_g^+, {}^1\Delta_g^-, {}^1\Delta_g(2), {}^1\Gamma_g$
	$NiCl_2$: $\cdots 8\sigma_g^2 7\sigma_u^2 \sigma_u^2 4\pi_u^4 2\pi_g^4 1\delta_g^4 3\pi_g^3 9\sigma_g^1$	${}^3\Pi_g$
$9\sigma_g^{-1}$	$\cdots 1\delta_g^4 3\pi_g^3$	${}^2\Pi_g$
$3\pi_g^{-1}$	$\cdots 1\delta_g^4 3\pi_g^2 9\sigma_g^1$	${}^4\Sigma_g^-, {}^2\Sigma_g^+, {}^2\Sigma_g^-, {}^2\Delta_g$
$1\delta_g^{-1}$	$\cdots 1\delta_g^3 3\pi_g^3 9\sigma_g^1$	${}^4\Pi_g, {}^4\Phi_g, {}^2\Pi_g(2), {}^2\Phi_g(2)$

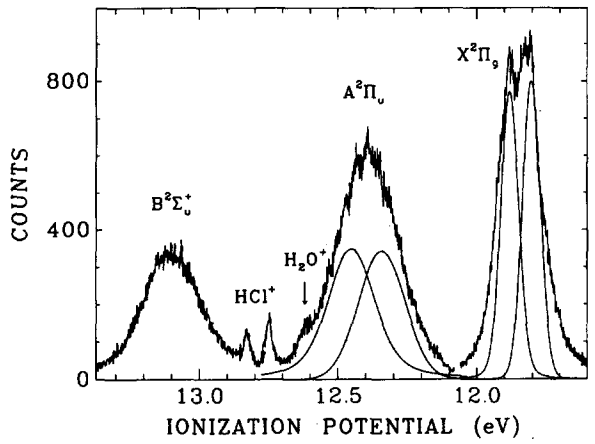

FIG. 3. The He I photoelectron spectrum from the $2\pi_g$, $4\pi_u$, and $7\sigma_u$ orbitals of $ZnCl_2$. Gaussians were fitted to the $A\ ^2\Pi_u$ band and are plotted in the spectrum to show the spin–orbit components.

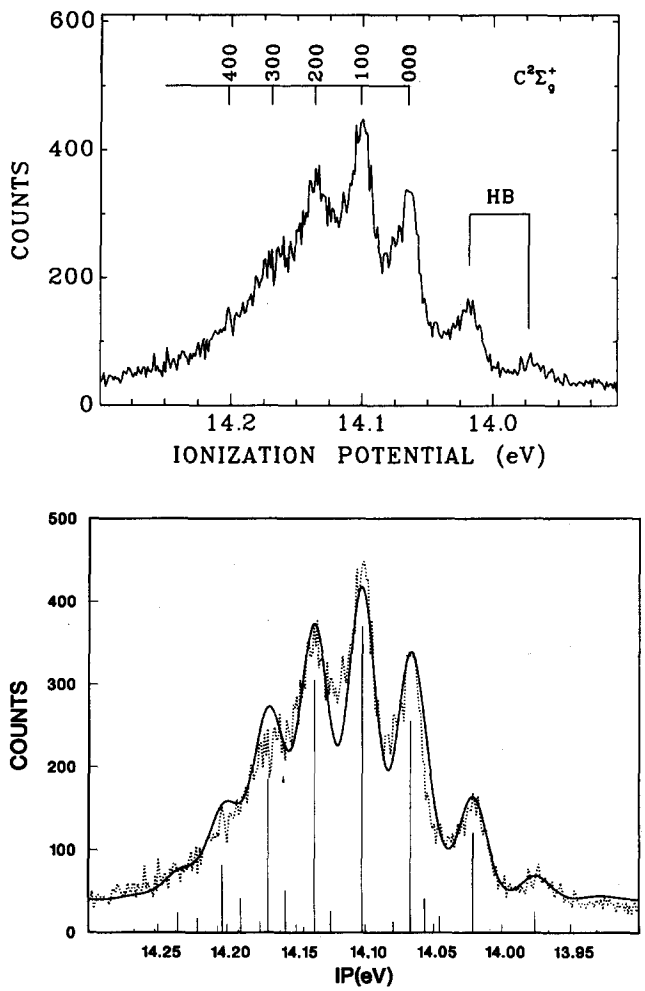

FIG. 4. (a) The He I photoelectron spectrum from the $9\sigma_g$ orbital of $ZnCl_2$, with the vibrational assignments. The vibrational levels are labeled with the ν_1, ν_2, and ν_3 vibrational quantum numbers. HB stands for the hot band transitions. (b) Comparison of a Franck–Condon factor calculation with the $C\ ^2\Sigma_g^+$ state experimental spectrum of $ZnCl_2^+$. The individual lines are the calculated Franck–Condon factors, each of which is convoluted with a Gaussian (0.024 eV width) to compare to the experimental spectrum (— calculated, ··· experimental).

ture in the spectrum if the vibrational frequencies do not change very much in the molecular ion.

Figures 3–5 illustrate the photoelectron spectrum of $ZnCl_2$ obtained in the current study. Figure 3 shows the three bands from the $7\sigma_u$, $4\pi_u$, and $2\pi_g$ orbitals. Figures 4 and 5 show the spectrum of the $9\sigma_g$ and the d orbitals, respectively. Spin–orbit splitting is partly resolved in the $X\ ^2\Pi_g$ band, while the two spin–orbit components in the $A\ ^2\Pi_u$ band are completely overlapped. This is because the $4\pi_u$ orbital is a bonding orbital and has a broader Franck–Condon envelope. Two Gaussians were fitted to the broad band and are plotted in Fig. 3 to show the two spin–orbit components. The spin–orbit splittings here are comparable to that in Cl_2^+.[37] The overlappings of the two spin–orbit components in these two bands apparently tends to smear out the vibrational structures, which are only partially resolved. For the $X\ ^2\Pi_g$ band, the ν_2 mode was observed to be excited with frequencies of about 240 and 260 cm^{-1} for the $^2\Pi_{g3/2}$ and $^2\Pi_{g1/2}$ components, respectively. For the $A\ ^2\Pi_{u3/2}$ band, two frequencies of 360 and 280 cm^{-1} are discernible. These should be due to the ν_1 and ν_2 modes, respectively. For the $A\ ^2\Pi_{u1/2}$ component, only a frequency of 280 cm^{-1}, corresponding to the ν_2 mode, can be recognized at the high ionization energy side. It is likely that the ν_1 mode was also excited with its features getting buried in the other spin–orbit component. These vibrational structures are indicated in Fig. 3.

A broad and featureless band was observed for the $B\ ^2\Sigma_u^+$ state, as can be seen from Fig. 3. It is surprising that no vibrational structure was resolved in this band, since there is no complication from the spin–orbit effect. This could, in principle, arise from either of two factors. The first one is lifetime broadening. This would mean that the $B\ ^2\Sigma_u^+$ state is unbound, which is not likely. More probably, the vibrational frequencies become smaller in the $B\ ^2\Sigma_u^+$ state and all three vibrational modes got strongly excited. This would produce a very congested and featureless band such as the one observed. If this is the case, even higher resolution might resolve vibrational structures in this band.

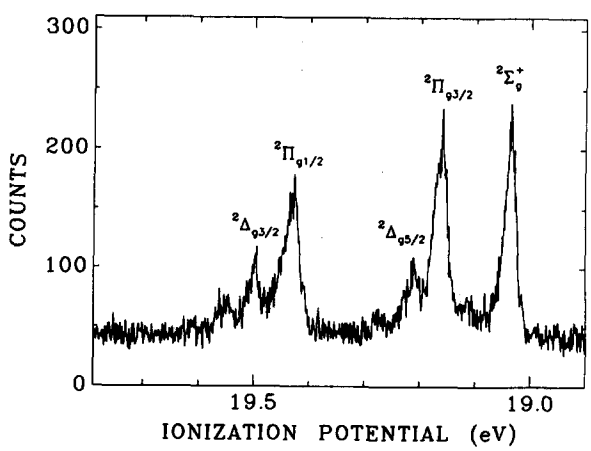

FIG. 5. The He I photoelectron spectrum from the Zn $3d$ orbitals ($8\sigma_g$, $2\pi_g$ and $1\delta_u$) of $ZnCl_2$, with the assignments.

TABLE III. Ionization potentials (eV) and assignments of the $C\,^2\Sigma_g^+$ state of $ZnCl_2^+$.

Ionization potential	Assignment[a]
13.975 (6)	Hot band ($\nu_1'' = 2 \rightarrow \nu_1' = 0$)
14.020 (5)	Hot band ($\nu_1'' = 1 \rightarrow \nu_1' = 0$)
14.065 (5)	0
14.101 (4)	1
14.136 (6)	2
14.170 (7)	3

[a] The ν_1 vibrational quantum number.

A beautifully resolved spectrum was observed for the $C\,^2\Sigma_g^+$ band, which is displayed in Fig. 4(a) with the assignment. The vibrational spacings between the first and second, and the second and third peaks are about 360 cm^{-1}, which is identical with the ground state ν_1 vibrational frequency (358 cm^{-1}).[36] Thus, the first two peaks are assigned to hot band transitions. The rest of the spectrum is assigned to a ν_1 vibrational progression. From Fig. 2, it is seen that the σ_g orbital is mainly a symmetric combination of the Cl $3p_z$ orbitals. So, it is not surprising that the ν_1 symmetric stretching mode was excited in the $C\,^2\Sigma_g^+$ state. The vibrational spacings, however, are considerably smaller than that in the neutral ground state, indicating the strongly bonding character of the σ_g orbital. The ionization potentials and the assignments of the $C\,^2\Sigma_g^+$ state are given in Table III.

A Franck–Condon factor calculation was performed to simulate the observed vibrational structure in the $C\,^2\Sigma_g^+$ state. Figure 4(b) shows a comparison between the calculated and experimental spectra. A Morse potential was employed in the calculation, which was done similarly as our previous calculations on diatomics.[18,19] From the calculation, we estimated a vibrational temperature of 350(50) K. The ν_1 vibrational frequency was found to be 290(8) cm^{-1}. More importantly, we obtained a Zn–Cl bond length increase of 0.095(5) Å with respect to the neutral ground state. The spectroscopic constants of the $C\,^2\Sigma_g^+$ state are given in Table IV together with the other states of $ZnCl_2^+$.

The spectrum of the 3*d* region of $ZnCl_2$ is shown in Fig. 5. Bancroft *et al.*[27] and others[24] have studied this part of the spectrum extensively, to probe the bonding characters of the 3*d* orbitals in Zn. They were the first to resolve the two spin–orbit components of the $^2\Pi_g$ and $^2\Delta_g$ states. The current spectrum is in good agreement with the previous studies, but with a better resolution. One difference is that there do not appear to be any sizable vibrational excitations, in contrast to the assignment by Bancroft *et al.* The extra feature at about 19.55 eV and the less visible feature at about 19.28 eV cannot be assigned to any vibrational levels, because their spacings relative to the immediate peaks at the lower energy side are not close to any vibrational frequencies. Considering the nonbonding character of the *d* orbitals, the vibrational frequencies in the molecular ion should not be very different from those in the neutral ground state. Bancroft *et al.* attributed these features to vibrational excitations without giving any specific assignments.[27] It should be pointed out that they only observed these features in their He II (304 Å) spectrum, but not in the He I spectrum. Therefore, they may arise, e.g., from multielectron processes, as it has been pointed out that electron correlation effects are important in this molecule.[38] Thus, the spectrum in the 3*d* region is very sharp, with little or no apparent vibrational excitation. This

TABLE IV. Spectroscopic constants of $ZnCl_2^+$.

	IPa (eV)[a]	IPv (eV)[b]	A (eV)[c]	$\omega_e(\nu_1)$ (cm^{-1})	$\omega_e(\nu_2)$ (cm^{-1})	r_{Zn-Cl} (Å)[d]
$X\,^2\Pi_{g3/2}$		11.802 (5)			240 (20)	
$^2\Pi_{g1/2}$		11.880 (5)	0.078		260 (20)	
$A\,^2\Pi_{u3/2}$		12.341 (10)		(360)	(280)	
$^2\Pi_{u3/2}$		12.451 (10)	0.110		(280)	
$B\,^2\Sigma_u^+$		13.103 (15)				
$C\,^2\Sigma_g^+$	14.065 (5)	14.101 (5)		290 (8)		2.145
3*d* bands						
$D\,^2\Sigma_g^+$		19.037 (5)	19.037 (5)			
$E\,^2\Pi_{g3/2}$		19.163 (5)	19.163 (5)			
$^2\Pi_{g1/2}$		19.434 (5)	19.434 (5)	0.271		
$F\,^2\Delta_{g5/2}$		19.213 (6)	19.213 (6)			
$^2\Delta_{g3/2}$		19.499 (6)	19.499 (6)	0.286		

[a] Adiabatic ionization potentials.
[b] Vertical ionization potentials.
[c] Spin–orbit splitting parameters.
[d] Zn–Cl bond length. A bond length increase of 0.095(5) Å was obtained from the Franck–Condon factor calculation. The bond length in the neutral ground state is 2.05 Å from Ref. 7.

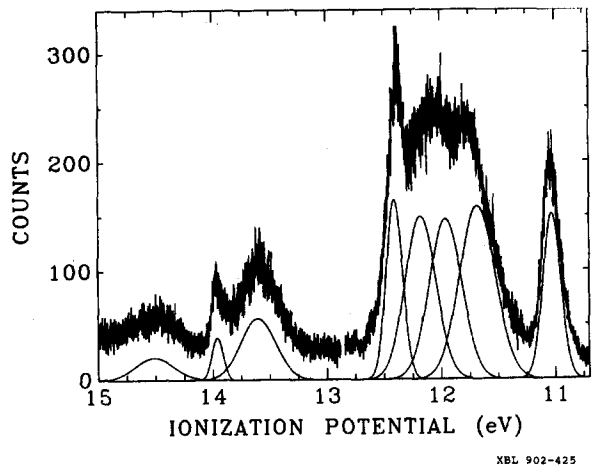

FIG. 6. The He I photoelectron spectrum of $MnCl_2$. Individual Gaussians were fitted to the observed bands and are plotted in the spectrum.

TABLE V. Ionization potentials (eV) and assignments for $MnCl_2$.

IP[a]	Assignment	Electronic term	FWHM (eV)[b]	Lee *et al.*[c]
11.03	$9\sigma_g^{-1}(3d)$	$^5\Sigma_g^+$	0.184	$9\sigma_g,3\pi_g$
11.68	$2\pi_g^{-1}$	$^7\Pi_g$	0.367	$4\pi_u,2u_g,7\sigma_u$
11.96	$4\pi_u^{-1}$	$^7\Pi_u$	0.332	(did not
12.18	$7\sigma_u^{-1}$	$^7\Sigma_u^+$	0.314	specify)
12.40	$3\pi_g^{-1}(3d)$	$^5\Pi_g$	0.160	
13.60	$8\sigma_g^{-1}$	$^7\Sigma_g^+$	0.360	$1\delta_g,8\sigma_g$
13.96	$1\delta_g^{-1}(3d)$	$^5\Delta_g$	0.115	(did not resolve)
14.51	$8\sigma_g^{-1}$	$^5\Sigma_g^+$	0.396	Satellite?

[a] Vertical ionization potentials, uncertainty = ± 0.01 eV.
[b] Full width at half-maximum of the fitted Gaussian.
[c] Reference 17.

is in accord with the expectation that the $3d$ orbitals of Zn are core-like, with little bonding capability.

The ionization potentials and the derived spectroscopic constants from the current study of $ZnCl_2^+$ are summarized collectively in Table IV.

C. $MnCl_2$

The photoelectron spectrum of $MnCl_2$ is shown in Fig. 6. The very low value of the bending frequency of $MnCl_2$ makes it impossible for us to resolve any vibrational structure. There are no gas phase measurements of the bending frequency available, but Thompson and Carlson[3] measured it as 83 cm^{-1} in an argon matrix: such a small value is beyond our current experimental resolution. Both hot band transitions, from thermal population of the ν_2 mode in the ground state, and excitation of this mode in the final state accompanying the photionization process would smear out any vibrational structure. Vibrational cooling in a supersonic expansion is relatively inefficient, and there should be a substantial thermal population of the low-frequency bending mode in our experiment.

For the spectral assignment, Lee *et al.*[17] used intensity differences between He I (584 Å) and He II (304 Å) spectra to identify features from the d orbitals. It was assumed that the d orbitals have an enhanced ionization cross section at the He II photon energy. In Fig. 6, we have fitted each observed band with a Gaussian, also plotted. There are three relatively sharp bands at ionization energies of 11.03, 12.40, and 13.96 eV. Two of these bands (11.03 and 13.96 eV) were assigned as being the d orbitals by Lee *et al.* They observed no definite intensity enhancement of the 12.40 eV peak in their He II spectrum, and did not assign this band to the d orbitals. However, from the sharpness of the band at 12.40 eV, we tentatively assign it as arising from the d orbitals. This illustrates one of the advantages of having high resolution. In the three previous investigations[15–17] at lower resolution, this assignment could not be made from the spectral width.

After identifying the bands arising from the d orbitals, we should easily be able to assign the rest of the bands from the ligands by analogy with the $ZnCl_2$ spectrum discussed in the above section. However, there is an extra band at 14.51 eV, which Lee *et al.* could not assign. They speculated that it was a satellite band. Lee *et al.*[17] did an *ab initio* molecular orbital calculation on $MnCl_2$ along with their experimental study. Although the overall accuracy of the calculation was not high enough to assign the spectrum, they found a remarkably large spin–spin splitting for the ionization of the $8\sigma_g$ orbital ($\sim$1 eV), but only very small spin–spin splittings for the ionizations of the other ligand orbitals. Based on this, we assign this extra band at 14.51 eV to be the low-spin state from ionization of the $8\sigma_g$ orbital. The high-spin band should be the one at 13.60 eV. The three bands at ionization energies of 11.68, 11.96, and 12.18 eV are assigned to be from the $2\pi_g$, $4\pi_u$, and $7\sigma_u$ orbitals, respectively. It is natural to assign the three bands from the d orbitals at 11.03, 12.40, and 13.96 eV to be from the $9\sigma_g$, $3\pi_g$, and $1\delta_g$ orbitals, respectively. The overall assignments, the ionization energies, and the band widths from the Gausian fitting are all tabulated in Table V. The assignments by Lee *et al.* are also given in Table V for comparison.

With reference to Table II, how do we explain the fact that there are only three bands observed for the ionizations of the d orbitals, much fewer than shown here? We notice that, for a one-electron transition, the spin selection rule says

$$S_i = S_f \pm 1/2,$$

where S_i is the initial spin in the neutral molecule, and S_f the final spin in the cation. The free photoelectron can carry either up or down spin. In $MnCl_2$, the five d electrons are all parallel to each other, giving the $^6\Sigma_g^+$ ground state. From the spin selection rule, only quintet states are allowed in a strictly one-electron transition. From Table II, there are only three allowed final quintet states, arising from each of the three d orbitals, in excellent agreement with our experimental observation. However, it is well known that electron correlation effect is strong in this open-shell system, resulting in multielectron processes, which would give rise to the other terms listed in Table II. This notwithstanding, multie-

lectron transitions usually have much smaller cross sections, and may have eluded the experimental observation. For the ionizations of the ligand orbitals, both septet and quintet states are allowed. As mentioned above, only for the $8\sigma_g$ orbital both low-spin and high-spin states were explicitly observed, and the spin–spin splittings for the other three ligand orbitals may be too small to be resolved experimentally.

We can gain additional insight into the $MnCl_2$ spectrum by considering the ionic limit, $Cl^-Mn^{2+}Cl^-$, for the ground state, in which Mn^{2+} has the free-ion character ($3d^5$; ^6S) of a high-spin half-filled shell, and the chlorine ions have filled $3p^6$ shells. In this model, removal of a $3d$ electron can only lead to a quintet final state. Crystal field theory leads unambiguously to the orbital order $9\sigma_g^{-1}$; $3\pi_g^{-1}$; $1\delta_g^{-1}$ for the $3d^{-1}$ final states through repulsive interaction with the chlorine ions. In the case of chlorine $3p$ ionization, it is helpful to consider a small degree of covalency. Only the $8\sigma_g$ combination of $3p_z$ orbitals can form a bond of reasonable strength (Fig. 2), and this orbital will clearly have the highest binding energy because the $3p_z$ orbitals both form a bonding combination and overlap with the attractive potential of the Mn^{2+} ion. The order, $7\sigma_u$; $4\pi_u$, $2\pi_g$, is also expected on similar arguments, as are the similar binding energies of these orbitals and their separation from the $8\sigma_g$ orbital. Thus, the large multiplet splitting occurred only in the $8\sigma_g$ orbital, because only the $8\sigma_g$ orbital has any appreciable density across the Mn^{2+} ion, facilitating large exchange integrals. In fact, the two peak ($^7\Sigma_g^+ - {}^5\Sigma_g^+$) multiplet pattern is strongly similar to the two peak ^7S–^5S pattern, well-known[39] in the $3s$ photoelectron spectrum of ionic Mn^{2+}, in which a $3s$ electron couples to the ($3d^5$; ^6S) shell through exchange, parallel to form ^7S and antiparallel to form ^5S. The smaller splitting in $MnCl_2$ is expected because the $8\sigma_g$ orbital cannot overlap with the Mn $3d$ shell as much as a Mn $3s$ electron. Even the width and lower (than statistical, 5:7) relative intensity of the $^5\Sigma_g^+$ peak is analogous, probably arising from electron correlation.[40]

D. $NiCl_2$

The spectrum of $NiCl_2$ is shown in Fig. 7, with the Gaussian fit plotted underneath each observed band. The ground state of $NiCl_2$ also has a very low bending vibrational frequency (85 cm^{-1}),[3] so no vibrational structure could be resolved. It is remarkable that four relatively narrow bands were resolved at low ionization energy. In all the previous investigations,[15–17] only one band was resolved in the same energy range. Evidently these four bands should be from the d orbitals, on the basis of their small band widths. It is noticed that there is some nitrogen inpurity from the background at high ionization energy. There are no other sharp bands in the entire spectrum, so the first four bands are apparently the only features from the d orbitals. The rest of the spectrum can be assigned by analogy with those of $ZnCl_2$ and $MnCl_2$, as shown in Table VI.

TABLE VI. Ionization potentials (eV) and assignments for $NiCl_2$.

IP[a]	Assignment	Electronic term	FWHM (eV)[b]	Lee *et al.*[c]
11.24	$9\sigma_g^{-1}(3d)$	$^2\Pi_g$	0.166	$9\sigma_g, 3\pi_g, 1\delta_g$
11.40	$3\pi_g^{-1}(3d)$	$^4\Sigma_g^-$	0.135	(Only resolved
11.56	$1\delta_g^{-1}(3d)$	$^4\Phi_g$	0.183	one band)
11.76	$1\delta_g^{-1}(3d)$	$^4\Pi_g$	0.150	
12.08	$2\pi_g^{-1}$	$^4\Delta_g$	0.322	$4\pi_u, 2\pi_g, 7\sigma_u$
12.60	$4\pi_u^{-1}$	$4\Delta_u$	0.352	(did not
13.00	$7\sigma_u^{-1}$	$^4\Pi_u$	0.302	specify)
13.70	$8\sigma_g^{-1}$	$^4\Pi_g$	0.450	$8\sigma_g$
15.25	$8\sigma_g^{-1}$	$^2\Pi_g$	0.400	$3\pi_g$, Satellite?

[a] Vertical ionization potentials, uncertainty = ±0.01 eV.
[b] Full width at half-maximum of the fitted Gaussian.
[c] Reference 17.

An expanded portion of the d region is plotted in Fig. 8. Only four components are evident, by either visual inspection or curve-fitting. Additional peaks could be present, either coincident in energy or with low intensity. In associating these peaks to the eleven possible final states listed in Table II, there are many possibilities. In none of the previous work[15–17] has any of these components been resolved. We make the very tentative assignment shown in Fig. 9. This

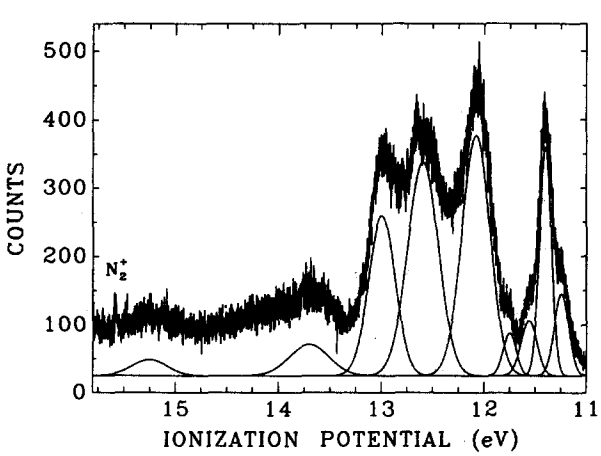

FIG. 7. The He I photoelectron spectrum of $NiCl_2$. Individual Gaussians were fitted to the observed bands and are plotted in the spectrum.

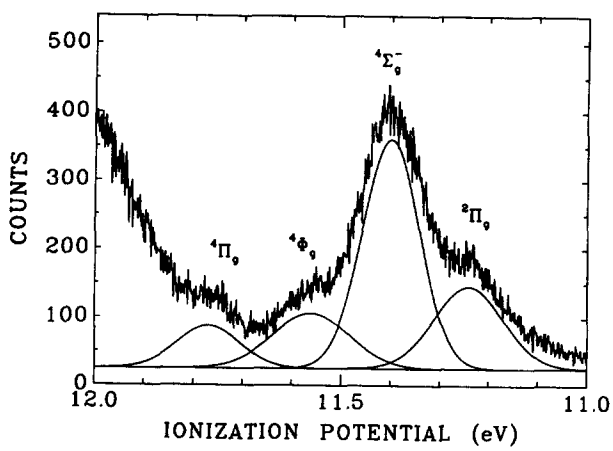

FIG. 8. An expanded portion of the He I photoelectron spectrum of the d bands region of $NiCl_2$, with the assignments and the individual Gaussians.

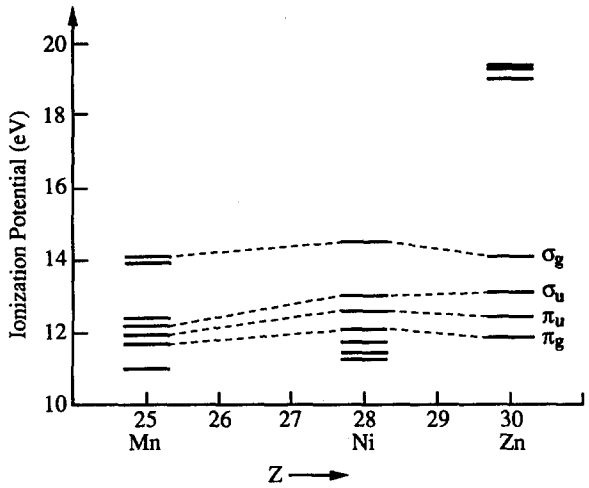

FIG. 9. Correlation diagram showing the valence orbital ionization potentials of $MnCl_2$, $NiCl_2$, and $ZnCl_2$. The *d* orbitals are not labeled.

TABLE VII. Vertical ionization potentials (eV) of the ligand orbitals and the *d* orbitals of $ZnCl_2$, $MnCl_2$, and $NiCl_2$.[a]

	Ionization potentials of the ligand orbitals			
	π_g	π_u	σ_u	σ_g
$ZnCl_2$	11.84	12.40	13.10	14.10
$NiCl_2$	12.07	12.60	13.01	14.47
$MnCl_2$	11.68	11.90	12.18	14.06
	Ionization potentials of the *d* orbitals			
	σ_g	π_g	δ_g	
$ZnCl_2$	19.04	19.30	19.35	
$NiCl_2$	11.24	11.40	11.70	
$MnCl_2$	11.03	12.41	13.96	

[a] In cases where there are spin–orbit or spin–spin splittings, an average value was taken as the ionization potential of the orbital.

assignment is neither firm nor unique. Its basis is as follows: we assume that photoionization, which removes a *d* electron from the triplet ground state of $NiCl_2$, will access any of the doublet or quartet final states of $NiCl_2^+$, given in Table II, for which $S_f = S_i \pm 1/2$. We assume further that some intensity is observed in ionization from each of the *d* orbitals, $9\sigma_g$, $3\pi_g$, and $1\delta_g$. Finally, we invoke a "weak form" of a high-spin propensity rule. That is, the highest-spin final states will appear to be enhanced relative to low-spin states. There are two firm reasons for this. First, the $(2S+1)$ spin multiplicity favors high-spin states. Second, electron correlation effects tend to distribute the intensity of photoelectron transitions to low-spin states over several peaks, reducing the intensity in the "main" peak. A clear example of this is in the photoionization of Mn^{2+} in a solid.[40]

In applying these assumptions, we note from Table II that the ionization of the $9\sigma_g$ orbital results in only one state ($^2\Pi_g$), the ionization of the $3\pi_g$ orbital leads to only one state with maximum multiplicity ($^4\Sigma_g^-$), and the ionization of the $1\delta_g$ orbital produces two states with maximum multiplicity ($^4\Phi_g$ and $^4\Pi_g$). According to the Hund's rules, the $^4\Pi_g$ state should have higher energy than the $^4\Phi_g$ state. So, the four bands from the *d* orbitals can be very tentatively assigned as shown in Fig. 9 and given in Table VI. Also given in Table VI are all the ionization energies and the assignments and the band widths from the Gaussian fittings, together with the assignments by Lee *et al.*[17] for comparison.

E. DISCUSSION

The photoelectron spectroscopy of the open-shell transition metal molecules is apparently very complicated. Evidently, not all the final states arising from an open-shell electron configuration would be observed experimentally. In the one-electron transition, first of all, the spin selection rule is obeyed. Even within the spin selection rule, we still found that there was a propensity toward high-spin final states in $NiCl_2^+$. The states with low spin and the states arising from electron correlations may have much smaller cross sections, and require much higher signal level to be observed. The fact that these were low signal experiments implied that there were many final states sharing the oscillator strength, and only the ones with large enough cross sections were experimentally observed. These may well apply to the transition metal cluster systems, where a large number of final states are expected from their open-shell nature, and caution must be taken to interpret the observed spectra. Quantum chemical calculations of the final state energy levels and partial cross sections would be very helpful.

Another question concerns spin–orbit splitting in the spectra of $MnCl_2$ and $NiCl_2$. For the ligand bands, the spin–orbit components must be contained in one band, based on the bandwidths and by comparison with the spectrum of $ZnCl_2$. For the bands of the *d* orbitals, it is also possible that the two spin–orbit components are contained in each band because the spin–orbit splitting parameters are comparable to the bandwidths. A different explanation could be offered for $NiCl_2$ if its ground state configuration was assumed to be closed-shell ($\cdots 1\delta_g^4 3\pi_g^4 9\sigma_g^0$). This configuration would yield the correct number of final states including the spin–orbit splittings, as shown in the following:

$$\cdots 1\delta_g^4 3\pi_g^4 (^1\Sigma_g^+) \rightarrow \cdots 1\delta_g^4 3\pi_g^3, \quad ^2\Pi_g \rightarrow {}^2\Pi_{g3/2}, {}^2\Pi_{g1/2}$$
$$\rightarrow \cdots 1\delta_g^3 3\pi_g^4, \quad ^2\Delta_g \rightarrow {}^2\Delta_{g5/2}, {}^2\Delta_{g3/2}.$$

The observed four *d* bands could be assigned to the above four spin–orbit components, and this even yields reasonable spin–orbit splitting parameters, 0.16 eV for the $^2\Pi_g$ state, and 0.20 eV for the $^2\Delta_g$ state. Indeed, two previous investigations[15,16] have assumed this ground state configuration for $NiCl_2$, although only one *d* band was resolved in these studies. Unfortunately, this ground state configuration of $NiCl_2$ is in apparent conflict with previous optical absorption studies[4–6] which concluded that the ground-state configuration of $NiCl_2$ should be $\cdots 1\delta_g^4 3\pi_g^3 9\sigma_g^1 (^3\Pi_g)$. Therefore, the closed-shell configuration cannot be taken for the spectral assignments of $NiCl_2$.

In Table VII are given all the orbital ionization energies of $ZnCl_2$, $NiCl_2$, and $MnCl_2$. In cases where there are spin–

orbit or spin–spin splittings, an average was taken as the orbital ionization energy. A correlation diagram of these orbital ionization energies is shown in Fig. 9. It is seen that the ligand orbital ionization energies of $NiCl_2$ are similar to that of $ZnCl_2$, while that of the $MnCl_2$ ligand orbital ionization energies show a slightly different pattern. It is known that the metal–ligand bonding in $ZnCl_2$ is primarily electrostatic. This suggests that the metal–ligand interaction is stronger in $MnCl_2$ than in $NiCl_2$, that is, there is more covalent character in the bonding of $MnCl_2$ than in that of $NiCl_2$. The ligand field splittings of the *d* orbitals support this view. While the splittings in $MnCl_2$ are very large, they are quite small in $NiCl_2$, being very close to that in $ZnCl_2$.

It is also instructive to examine the *d* orbital bandwidths. In the spectrum of $ZnCl_2$ shown in Fig. 5, the bands are very narrow, on the order of the instrumental resolution, with little vibrational excitation. However, the *d* band widths are considerably broadened in $MnCl_2$ and $NiCl_2$. The broadening cannot be fully explained by spin–orbit and thermal effects. There must be some vibrational excitations, most likely of the low frequency bending mode, suggesting significant covalent bonding between the central metal atom and the ligands in $MnCl_2$ and $NiCl_2$ in comparison with $ZnCl_2$. This supports the general conviction that the participation in chemical bonding of the 3*d* orbitals in the first row transition metal elements weakens from left to right in the Periodic Table.

IV. SUMMARY

We have measured the high resolution He I (584 Å) photoelectron spectra of $ZnCl_2$, $MnCl_2$, and $NiCl_2$. Vibrational structure was resolved in the $ZnCl_2$ spectrum A single ν_1 vibrational progression was observed in the $C\,^2\Sigma_g^+$ state of $ZnCl_2^+$. A simple Franck–Condon factor calculation with a Morse potential simulated the spectrum very well and allowed us to estimate a vibrational temperature of 350(50) K for the $ZnCl_2$ molecules. A ν_1 vibrational frequency of 290(8) cm^{-1} and a Zn–Cl bond length increase of 0.095(5) Å were also derived from the calculation. Spin–orbit splitting was partly resolved in the $X\,^2\Pi_g$ state while the two spin–orbit components were heavily overlapped in the $A\,^2\Pi_u$ state. Vibrational structure was partially resolved in these two states. Five peaks were clearly resolved for the *d* orbitals including the spin–orbit effect, with little or no vibrational excitation.

No vibrational structure was resolved in the cases of $MnCl_2$ and $NiCl_2$ because of the very low bending frequencies in these two molecules. However, the high resolution was very helpful to identify the bands arising from the *d* orbitals, and their bandwidths yielded information about the bonding character. The much broader bandwidths indicated significant covalent bonding involvement of the 3*d* electrons. However, much fewer final states were observed than expected from their open-shell configurations. In $MnCl_2^+$, only three bands could be attributed to the *d* orbitals, which were assigned to the three highest-spin final states, for which there was no spin-flip (spin selection rule). Only four peaks could be clearly resolved in $NiCl_2^+$, which may be associated to the *d* orbitals. For assignment of these four states, a propensity toward high-spin states was proposed in addition to the spin selection rule. The spectra of the ligand orbitals in $MnCl_2^+$ and $NiCl_2^+$ are similar to that of $ZnCl_2^+$, except that the separation between the σ_g orbital and the other ligand orbitals increases in the order $MnCl_2 > NiCl_2 > ZnCl_2$, supporting the view that the covalent bonding character increases in the same order.

ACKNOWLEDGMENTS

The authors would like to acknowledge the referee for suggesting the assignment of the vibrational structure in the $C\,^2\Sigma_g^+$ state of $ZnCl_2^+$. L.S.W. wishes to thank Dr. P. A. Heimann and Professor E. R. Grant for valuable discussions. This work was supported by the Director, Office of Energy Research, Office of Basic Energy Sciences, Chemical Sciences Division of the U.S. Department of Energy under Contract No. DE-AC03-76SF00098.

[1] See for example, F. A. Cotton and G. Wilkinson, *Advanced Inorganic Chemistry*, 2nd ed. (Wiley, New York, 1966).
[2] G. E. Leroi, T. C. James, J. T. Hougen, and W. Klemperer, J. Chem. Phys. **36**, 1879 (1962).
[3] K. Thompson and K. D. Carlson, J. Chem. Phys. **49**, 4379 (1968).
[4] J. T. Hougen, G. E. Leroi, and T. C. James, J. Chem. Phys. **34**, 1670 (1961).
[5] C. W. DeKock and D. M. Gruen, J. Chem. Phys. **44**, 4387 (1966).
[6] A. B. P. Lever and B. R. Hollebone, Inorg. Chem. **11**, 2183 (1972).
[7] I. Hargittai and J. Tremmel, Coord. Chem. Rev. **18**, 257 (1976).
[8] A. Buchler, J. L. Stauffer, and W. Klemperer, J. Chem. Phys. **40**, 3471 (1964).
[9] L. Brewer, G. R. Somayajulu, and E. Brachett, Chem. Rev. **63**, 111 (1963).
[10] C. D. Garner, I. H. Hillier, and C. Wood, Inorg. Chem. **17**, 168 (1978).
[11] M. Costas and A. Garritz, Int. J. Quant. Chem., Quant. Chem. Symp. **13**, 141 (1979).
[12] W. von Niessen and L. S. Cederbaum, Mol. Phys. **43**, 897 (1981).
[13] I. Shim and K. A. Gingerich, J. Chem. Phys. **77**, 2490 (1982).
[14] G. G. Leopold and W. C. Lineberger, J. Chem. Phys. **85**, 51 (1986).
[15] J. Berkowitz, D. G. Streets, and A. Garritz, J. Chem. Phys. **70**, 1305 (1979).
[16] R. M. MacNaughton, J. E. Bloor, R. E. Sherrod, and G. K. Schweitzer, J. Electron Spectrosc. Relat. Phenom. **22**, 1 (1981).
[17] E. P. F. Lee, A. W. Potts, M. Doran, I. H. Hillier, J. J. Delaney, R. W. Hawksworth, and M. F. Guest, J. Chem. Soc. Faraday II **76**, 506 (1980).
[18] L.-S. Wang, B. Niu, Y. T. Lee, and D. A. Shirley, Chem. Phys. Lett. **158**, 297 (1989).
[19] L.-S. Wang, B. Niu, Y. T. Lee, D. A. Shirley, and K. Balasubramanian, J. Chem. Phys. **92**, 899 (1990).
[20] L.-S. Wang, J. E. Ruett-Robey, B. Niu, Y. T. Lee, and D. A. Shirley, J. Electron. Spectrosc. Relat. Phenom. **51**, 513 (1990).
[21] C. W. Bauschlicher, Jr. (private communication).
[22] G. W. Boggess, J. D. Allen Jr., and G. K. Schweitzer, J. Electron Spectrosc. Relat. Phenom. **2**, 467 (1973).
[23] J. Berkowitz, J. Chem. Phys. **61**, 407 (1974).
[24] A. F. Orchard and N. V. Richardson, J. Electron Spectrosc. Relat. Phenom. **6**, 61 (1975).
[25] E. P. F. Lee and A. W. Potts, J. Electron Spectrosc. Relat. Phenom. **22**, 247 (1981).
[26] D. J. Bristow, G. M. Bancroft, and J. S. Tse, Chem. Phys. **75**, 263 (1983).
[27] G. M. Bancroft, D. J. Bristow, and J. S. Tse, Chem. Phys. **75**, 277 (1983).
[28] J. H. Canterford and R. Colton, *Halides of the First Row Transition Metals* (Interscience, New York, 1968).
[29] D. W. Rice and N. W. Gregory, J. Phys. Chem. **72**, 3361 (1968).
[30] F. J. Keneshea and D. Cubicciotti, J. Chem. Phys. **40**, 191 (1964).
[31] R. C. Schoomaker, A. H. Friedman, and R. F. Porter, J. Chem. Phys. **31**, 1586 (1959).

[32]J. E. Pollard, D. J. Trevor, Y. T. Lee, and D. A. Shirley, Rev. Sci. Instrum. **52**, 1837 (1981).
[33]J. H. Van Vleck and A. Sherman, Rev. Mod. Phys. **7**, 167 (1935).
[34]A. D. Liehr, J. Chem. Educ. **39**, 135 (1962).
[35]G. Herzberg, *Molecular Spectra and Molecular Structure I. Spectra of Diatomic Molecules*, 2nd ed. (Van Nostrand Reinhold, New York, 1950), p. 333.
[36]A. Loewenschuss, A. Ron, and O. Schnepp, J. Chem. Phys. **49**, 272 (1968).
[37]H. van Lonkhuyzen and C. A. De Lange, Chem. Phys. **89**, 313 (1984).
[38]L. S. Cederbaum, W. Domcke, J. Schirmer, and W. von Niessen, Adv Chem. Phys. **65**, 115 (1986).
[39]C. S. Fadley, D. A. Shirley, A. J. Freeman, P. S. Bagus, and J. V. Mallow Phys. Rev. Lett. **23**, 1397 (1969).
[40]S. P. Kowalczyk, L. Ley, R. A. Pollack, F. R. McFeely, and D. A. Shirley Phys. Rev. B **7**, 4009 (1973).